EXPLORING THE COMBUSTION CHARACTERISTICS OF TURBULENT PREMIXED AMMONIA/HYDROGEN/AIR FLAMES VIA DTF MODEL-BASED LARGE EDDY SIMULATION

by

Ping WANG[a,b*], Zeyu ZHANG[a], Zhengchun YANG[a], Subhajit ROY[a], Weijia QIAN[a], and Kang CHENG[a]

[a] Institute for Energy Research, Jiangsu University, Zhenjiang, Jiangsu, China
[b] State Key Laboratory of Clean Energy Utilization, Zhejiang University, Hangzhou Zhejiang, China

Original scientific paper
https://doi.org/10.2298/TSCI231123002W

This study aims to investigate the combustion characteristics of a premixed swirl flame for a fuel mixture made of NH_3 and H_2. The use of NH_3 and H_2 as carbon-free fuels in combustion systems can significantly reduce GHG emissions. Blending NH_3 with H_2 is a promising approach to enhance H_2 combustion safety and NH_3 combustion intensity. A 3-D large eddy simulation using a dynamically thickened flame (DTF) model was run in order to get extensive and multi-scale information regarding the flow and reacting field of a premixed swirl flame using a 50% NH_3 50% H_2 fuel blend. The findings indicate that whereas NO is created near the flame front, OH radicals are mostly synthesized in the inner re-circulation zone. The fuel-NO pathway, which is sensitive to flame temperature, is what causes NO to be produced. The flame position is where the re-circulation zone lies, and the total re-circulation strength is determined by the inner re-circulation strength. The prediction of NO concentration by large eddy simulations, considering heat loss, is closer to the experimental value. The chemically reacting network simulation can precisely estimate NO emission by considering the heat loss ratio and the re-circulation strength calculated by large eddy simulations. Overall, this study provides valuable insights into the combustion characteristics of an NH_3/H_2 fuel blend, which could contribute to the development of cleaner and more efficient combustion technologies. The findings of this study can be of great significance in the fields of sustainable energy and environmental protection.

Key words: *low carbon fuel, DTF model, NH_3 combustion, large eddy simulations, turbulent flame*

Introduction

It is now widely acknowledged that global warming, which is caused by CO_2 emissions, is an urgent problem. A sizable percentage of these emissions have been caused by fossil fuels, which constitute the main source of energy for industrial and human activity globally. As a result, the use of carbon-free fuels is necessary to reduce CO_2 emissions. To achieve this, significant research efforts are required in developing and implementing such fuels.

The unique feature of NH_3, which causes it to solely produce water and nitrogen as combustion byproducts when entirely burned, has recently drawn the attention of researchers.

* Corresponding author, e-mail: pingwang@ujs.edu.cn

Furthermore, NH_3 is a viable H_2 energy vector because its molecules can store an enormous amount of H_2, up to 17.7% [1]. The NH_3 has been used as a chemical fertilizer for more than a century, and the Haber-Bosch production method and distribution network for NH_3 are both well-established. A RES, such as solar energy, can also be used to create NH_3 today [2]. In addition its potential as a H_2 energy vector, NH_3 has a lot of appealing qualities as a fuel, including the ability to liquefy at low pressure (0.8 MPa) and ambient temperature [3]. This gives the transportation of NH_3 a significant safety and convenience advantage over other energy sources. As a result of its well-established production process and infrastructure, high H_2 storage capacity, and accessible and affordable fuel characteristics, NH_3 has enormous potential as a H_2 energy vector. The current developments in the ecologically friendly and sustainable synthesis of NH_3 further increase its appeal as an energy source for the future. A cleaner and more effective energy environment could result from continued research and development in this field, opening up new avenues for innovation and economic expansion.

Since the 1960's, there has been a lot of research on NH_3 combustion, as shown in several scientific publications [4-9]. For instance, Verkamp *et al.* [4] experimental investigation on the quenching distance revealed that, under stoichiometric conditions, NH_3-air displayed a quenching distance that was 3.5 times larger than propane. Additionally, the laminar burning velocity of NH_3-air mixtures is quite modest, peaking at 6-8 cm per seconds at an equivalency ratio of around 1.1 [5, 6]. Comparing this number to CH_4-air, it is approximately five times lower. It has been shown that the low laminar burning velocity prevents the utilization of both high inlet velocities and low inlet velocities to produce effective turbulent mixing and high combustion efficiency, respectively [7]. Additionally, because NH_3 contains a nitrogen atom, it may generate large amounts of nNO_x, which can be harmful [8, 9]. Therefore, the main difficulty in NH_3 combustion is achieving a stable flame and low NO_x emissions.

According to numerous scholarly articles [10-14], researchers have investigated the use of H_2 as an addition improve the lower combustion intensity of NH_3. An experimental investigation was undertaken by Han *et al.* [10] to determine whether mixing NH_3 and H_2 would boost the laminar burning velocity of NH_3-containing fuel. The study found that the best strategy to increase the laminar burning velocity of NH_3-containing fuel is to blend it with H_2. Additionally, it was discovered that fuel NO_x predominated, but thermal NO_x had a negligible impact on the burning of NH_3, H_2, and air [11]. Valera-Medina *et al.* [12, 13] performed experiments for the NH_3/H_2 blend at the gas turbine research center. Their findings showed that in lean conditions, NO_x emissions are substantial due to the excessive formation of OH and O radicals, whereas under rich combustion conditions, comparatively low NO_x emissions are possible due to the presence of unburned NH_3. In a laboratory-scale swirl and bluff-body stabilized burner, Franco *et al.* [14] tested the combustion of NH_3/H_2/air while altering the equivalence ratio and NH_3 content. They proposed that NO_x is generated close to the burner input and then eliminated, perhaps through selective non-catalytic reduction. Overall, these investigations indicate that the addition of H_2 may be a useful strategy for increasing NH_3 combustion intensity while also tackling the issue of NO_x emissions.

To employ NH_3-containing fuel in actual combustion equipment, it is essential to study the combustion characteristics of these fuels. The CFD has been identified as an efficient method for analyzing the behavior of different critical species and radicals within the chamber. As reported in [15-19], several research have been carried out to investigate the combustion of fuel containing NH_3 in different types of burners. In order to study the combustion of NH in a similar burner, Somarathne *et al.* [15] and Okafor *et al.* [16] used 3-D large eddy simulations (LES). They discovered that the addition of secondary air-flow can significantly minimize the

amount of NO emissions. The combustion of NH_3-containing fuel in the Cardiff University swirl burner has been numerically explored by a number of research groups, including Honzawa *et al.* [18], who compared the NO content for the combustion of an NH_3/CH_4 blend under adiabatic and non-adiabatic conditions. The findings demonstrated a good agreement between predicted values and experimental values using a non-adiabatic flamelet-generated manifold method. The impact of heat loss was also examined by Vigueras-Zuniga *et al.* [19] using RANS simulations. However, there is still a scarcity of studies that have focused on 3-D simulations of NH_3-containing fuel flames. Additionally, there has been little research examining the validity of turbulence combustion models, particularly the flamelet approach. Further studies are needed to develop a more comprehensive understanding of the combustion behavior of NH_3-containing fuels, which will facilitate the use of these fuels in practical combustion equipment.

In this study, LES was employed using the DTF model to validate the method by comparing the amount of NO produced. This study presents an investigation into the progression of the flame of a 50% NH_3/50% H_2 fuel mixture under lean premixed conditions in a swirl burner [20]. The flame structure was initially analyzed from the perspective of a 1-D simulation, followed by conducting LES under two types of confinement conditions. The DTF model, an extension of the artificially thickened flame model, which artificially thickens the flamelet, was used to characterize the flame structure using the LES grid.

The primary goals of this work are to offer new insights on combustion characteristics of NH_3-containing fuels and assess how well the DTF model predicts NO emissions. The accuracy of the simulations is confirmed by comparing the results with experimental data, which also helps to clarify the intricate physics underlying NH_3 combustion.

Numerical methods

Swirl burner and boundary condition

A LES with finite rate chemistry was carried out using the OpenFOAM platform [21] in order to acquire a thorough 3-D understanding of the flame structure at lean conditions for a 50% NH_3/50% H_2 fuel blend. An overview of the burner and grid design used in the simulation is shown in fig. 1. The details regarding this burner can be found in previous studies [20,

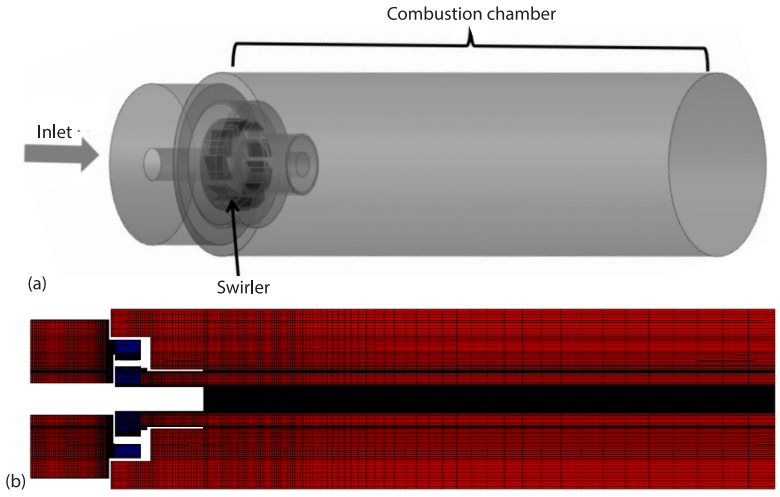

Figure 1. Overview of burner configuration and grid configuration; (a) burner configuration and (b) grid configuration

22]. The fuel blend used in this investigation was 50% NH_3 and 50% H_2 by volume, with air serving as the oxidizer. This fuel blend was chosen due to its ability to produce a good laminar burning velocity similar to CH_4 with near equivalent laminar burning velocity characteristics. Additionally, NO emissions were measured [22]. The NH_3/H_2/air mixture was supplied from the inlet with a constant equivalence ratio of 0.577. The wall condition was set to zero gradient for adiabatic wall, while for non-adiabatic wall conditions, the wall temperature was fixed at the average of the inlet temperature and adiabatic flame temperature, which was 950K. Table 1 provides a summary of the boundary conditions used for the initial validation. The entire combustion chamber is computed using a structured mesh, which is generated using ICEM. Due to the study's focus on thermal boundary conditions, the quality of the mesh near the wall is crucial. The mesh is refined near the wall, with the grid size in this region being much smaller than the boundary-layer thickness. This allows for a detailed resolution of the flow field structure near the wall when solving the boundary-layer.

Table 1. Boundary conditions

Operating pressure	1 atm	
Oxidiser [mol%]	O_2	21%
	N_2	79%
Fuel [mol%]	NH_3	50%
	H_2	50%
Mass-flow rate [gs^{-1}]	NH_3	0.800
	H_2	0.094
	Air	14.001
Inlet temperature	300 K	
Wall condition	Adiabatic, 950 K	

The dynamically thickened flame model and mechanism

The DTF model was proposed by Butler and O'Rourke [23]. This model modifies the exponential constants of the chemical reaction rate and thermal diffusion coefficient by a factor F. To enable the resolution of the flame on an LES grid, the thickening factor $F_{dyn} = F(n_{DTF})$ is varied from large values inside the reaction zone to unity away from the flame front. An efficiency function E that may overcome the reduction of flame response to the smallest turbulent motions during the thickening process has been developed by Angelberger *et al.* [24] and Colin *et al.* [25]. This function E depends on the thickening factor F, the length scale $\Delta e/\delta_L^0$, and the velocity $u'_{\Delta e}/S_L^0$ ratios where Δe is the combustion LES filter size, δ_L^0 – the laminar flame thickness, $u'_{\Delta e}$ – the subgrid scale rms velocity, and S_L^0 – the laminar burning velocity.

Three global variable parameters need to be predetermined when utilizing the DTF model to handle the interaction between turbulence and chemistry:

– global grid thickening coefficient, n_{DTF},
– laminar flame thickness, δ_L^0, and
– laminar burning velocity, S_L^0.

After 1-D premixed free propagated flame simulation, The δ_L^0 and S_L^0 are 1 mm and 0.126 m/s, respectively, following a simulation of a 1-D premixed free propagating flame. Wang *et al.* [26] employed the DTF model to study the CH_4/air flame with an equivalence ratio of 0.75 and 0.83 at the atmosphere. The analysis demonstrates that numerical results using the small thickening coefficient (n_{DTF} = 2.5~5) in the dynamic thickening process are in good agree-

ment with the experimental findings. Premixed CH_4/air laminar flame has a flame thickness in the range of 1-2 mm, which is comparable to the 50% NH_3/50% H_2 fuel blend's laminar flame thickness at $f = 0.577$ calculated previously. Hence, this paper uses the thickening coefficient proposed by Wang *et al.* [26] and adopts the thickening coefficient $n_{DTF} = 5$.

The non-linear chemical kinetics equations must be coupled to fluid dynamics and transport phenomena in order to simulate the combustion process. As this can be a time-consuming process, it is often necessary to use reduced mechanisms to minimize computational time. The NH_3/H_2 mechanism developed by Xiao *et al.* [27] is a good example of such a reduced mechanism. Excellent agreement in the laminar burning velocity is shown by this approach, which also requires a lot less computing time [28]. Therefore, the NH_3/H_2 mechanism, which consists of 24 species and 91 steps, was applied in this study to model the chemical kinetics.

The 1-D numerical studies

The 1-D premixed free propagating flame calculations were carried out with CANTERA [29] to better understand the flame structure. The CHEMKIN-PRO [30] was used to determine the impact of re-circulation strength and heat loss on the final NO emission. A chemical reactor network (CRN) approach was used to model the swirling flame with a re-circulation zone, as shown in fig. 2. The CRN used in this study consists of a hybrid perfectly stirred reactor (PSR), a plug flow reactor (PFR), and a partially stirred reactor (PaSR), which are composed of four sections. Two inlets were utilized to provide a 50% NH_3/50% H_2 fuel mixture and an air/water vapor mixture, while three PSR were employed to simulate the premixed zone, premixed flame, and central re-circulation zone. The post-flame region was modeled using a 1-D PFR with a length of 5 cm. The PaSR was designed to simulate the extinguishment/mixing zone of the main combustion products and secondary air-flow. The lean zone was simulated using the second PFR, which had an axial length of 5 cm. An NH_3/H_2 fuel mixture's main combustion zone typically has a residence duration of a few milliseconds, and the generation of NO_x there is not very sensitive to the residence time. As a result, the primary flame zone's residence time in this investigation was set at 1.5 ms. The two PFR employed in this investigation have sufficient 1-D length since the NO_x concentration rapidly drops in the front of the PFR and stabilizes in the back. The researchers were able to develop a thorough grasp of the combustion process and flame structure by utilizing these different methods.

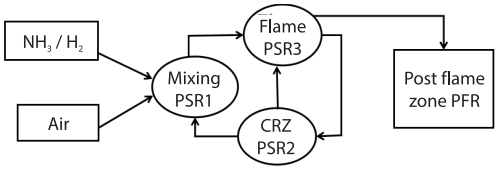

Figure 2. The PSR-PFR schematic

Results and discussion

The 1-D flame simulation using cantera

The 1-D structure of a laminar premixed flame at an equivalence ratio of 0.577 is depicted in fig, 3. The flame thickness is approximately 1 mm, and the flame temperature is about 1620 K. Since the flame temperature is below 1800 K, which is the critical temperature to generate thermal NO, fuel NO predominates in the ultimate NO emission. When the curves between NH_3 and H_2 are compared, it can be seen that H_2 reacts more quickly and produces a bigger reaction zone than NH_3 due to the higher H_2 diffusion and consumption rates. Additionally, as shown in fig. 3(a), the mole fraction of H_2 is somewhat higher than that of NH_3 during burning, most likely as a result of NH_3 breaking down into H_2. The NO mole fraction is approximately 0.0062 from the 1-D laminar numerical calculation. The formation of NO is sensitive

to the content of OH, O, and H radicals [31], which is consistent with the trend of OH, O, and H radicals and NO, as shown in fig. 3(b). The OH, O, and H radicals reach a peak near the flame front, and NO is also generated around the flame front. Moreover, the decomposition of NH_3 is related to the content of OH, O, and H radicals [32], with OH radicals playing the most important role. H_2 can improve the combustion properties of pure NH_3, most likely as a result of the reaction between H_2 and O_2 that produces the OH, O, and H radicals.

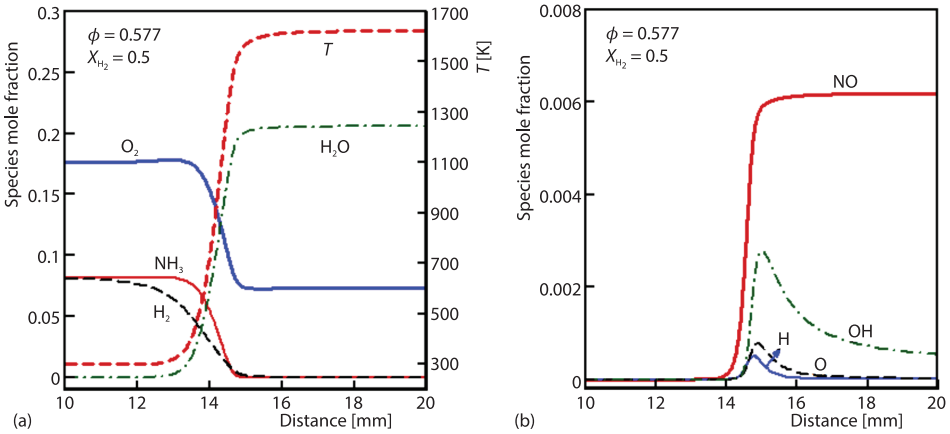

Figure 3. Predicted structure of a premixed laminar free propagated NH_3/H_2 flame at equivalent ratio of 0.577

The NO emissions are a major concern when using NH_3-containing fuel in practical combustion devices. Figure 4 illustrates the impact of re-circulation zone ratio and heat loss ratio on NO emissions. Figures 4(a) and 4(b) vary the re-circulation zone ratio under adiabatic conditions, while figs. 4(c) and 4(d) vary the heat loss ratio at a re-circulation zone ratio of 0.2. Increasing the re-circulation zone ratio and heat loss ratio can reduce the absolute NO production rate, resulting in a decrease in NO emissions. Figure 4(b) illustrates how the effect of the re-circulation zone ratio on the flame temperature and OH concentration can be disregarded. Thus, the increase in NO production rate and emissions is caused by the entrance of more flue gas into the re-circulation zone, leading to an increase in NO in the flame zone. On the other hand, increased heat loss decreases the concentration of OH radicals, which are reactants for NO formation, resulting in a reduction of NO emissions. Furthermore, as figs. 4(b) and 4(d) indicate, the flame temperature and OH mole fraction exhibit a positive correlation relationship.

Analysis of velocity field under large eddy simulation

Two hybrid computational meshes with 1.4 million (coarse) and 2.67 million (fine) cells each were generated to conduct a grid independence study. The unstructured cells were used in the swirl section, while structured cells were used in other parts of the mesh. Additionally, small cells were also provided to alleviate the turbulent eddies in the re-circulation zone around the axial area. The axial distribution diagram of burner temperature and NO mole fraction was simulated to ascertain the grid's appropriateness, as shown in fig. 5. There was a recurring pattern when the two grid sets were compared. In contrast to the coarse grid, the fine grid had a more erratic flame position. This phenomenon can be attributed to the fine grid's sensitivity to temperature and NO emissions. Considering the trade-off between calculation accuracy and speed, the fine grid was ultimately selected for this study.

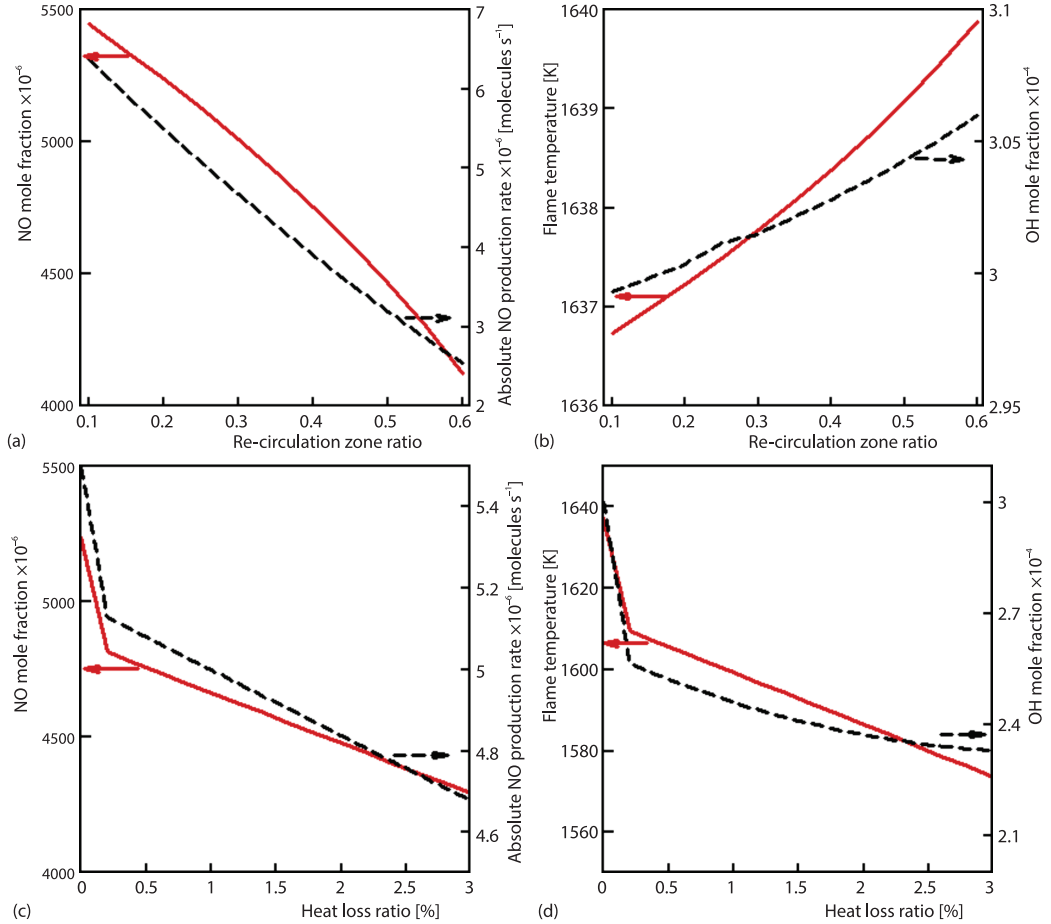

Figure 4. Effect of re-circulation zone ratio and heat loss ratio on NO emission, flame temperature and OH mole fraction

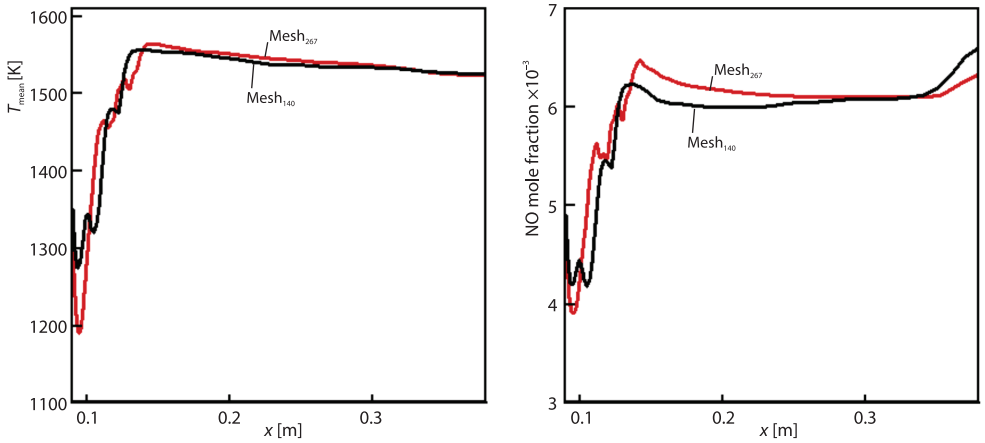

Figure 5. Comparison of calculated values for two sets of grids; (a) averaged temperature and (b) averaged NO mole fraction

In this study, an approach using 2-D cloud image slices and section position analysis was utilized to investigate the effect of heat loss on the combustion characteristics of NH_3/H_2 premixed flames. It is essential to clarify that the solid line represents the axial average velocity where the speed is zero. The re-circulation zone includes various components such as the internal re-circulation area (IRZ) and the external re-circulation area (ORZ) that is surrounded by the zero-gradient line. As shown in fig. 6, a significant phenomenon is observed where the free radicals and hot combustion gas are brought by re-circulation into the upstream region of the combustion chamber. This leads to the mixing of combustion and unburned gases in the return zone, thereby maintaining a continuous chemical reaction under the influence of a strong swirling flow. The re-circulation zone acts as a carrier of heat and mass, which plays a vital role in the overall combustion process. The detailed analysis of the re-circulation zone and its impact on the combustion process is critical for the optimal design and operation of practical combustors.

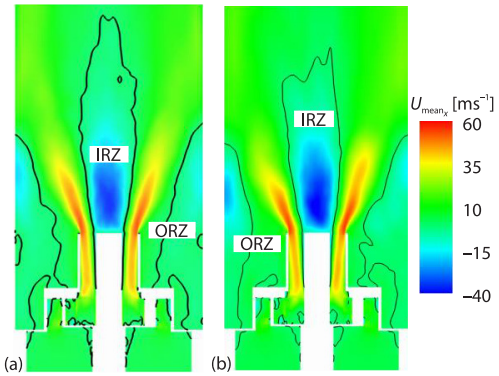

Figure 6. Comparison of axial average velocity at adiabatic and non-adiabatic wall conditions; (a) non-adiabatic axial average velocity and (b) adiabatic axial average velocity

Figure 7 displays the average temperature under two wall conditions to examine the impact of heat loss. The axial velocity averages of various sections along the radial direction are compared under two conditions: adiabatic condition (zero-gradient) and wall temperature of 950 K. The five axial distances correspond to the height from the flame root to the top (x = 0.09 m, 0.11 m, 0.13 m, 0.15 m, 0.17 m, 0.19 m). Several similarities between the two

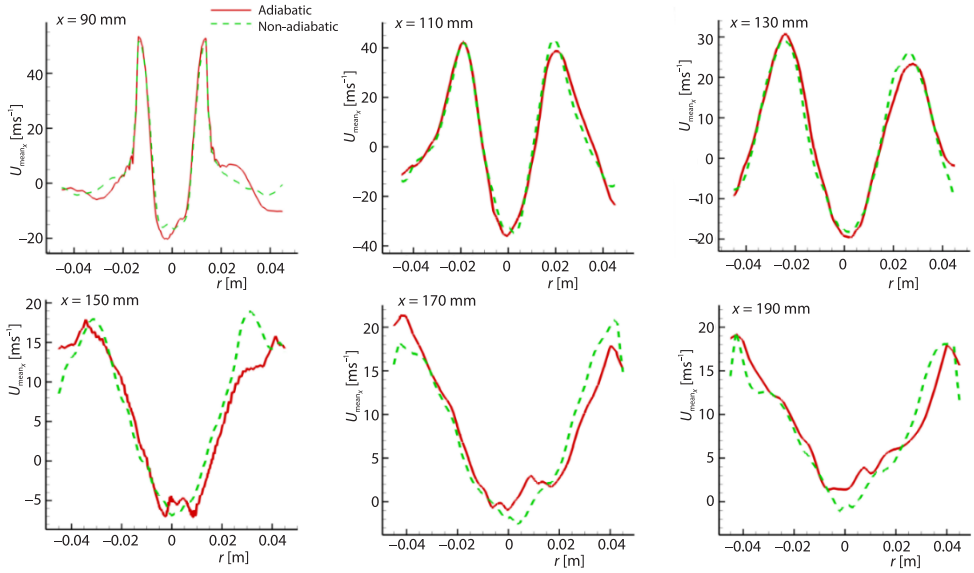

Figure 7. Comparison of the radial average velocity at different axial locations for non-adiabatic and adiabatic conditions, x = 90 mm, 110 mm, 130 mm, 150 mm, 170 mm, 190 mm

wall conditions can be observed. The average velocity at the flame center is nearly identical, but the velocity near the wall differs. As shown in fig. 6, the strength of the IRZ is significantly greater than that of the ORZ, indicating that the total re-circulation strength is determined by the internal re-circulation strength. As the flame develops downstream, the internal re-circulation increases, reaching the maximum value at the axial position of 0.11 m (in the middle of the flame) as the re-circulation speed decreases. Furthermore, the closer to the flame root, the greater the axial velocity gradient of the outer layer of the internal circulation zone, indicating that the shear layer mixing of fresh mixture and gas in the internal circulation zone is more intense.

Figure 7 shows that at the flame root (x = 90 mm), the reflux velocity is slightly increased under the diabatic condition. At x = 110 mm and x = 130 mm, there is almost no difference, which is caused by the influence of the central part of the flame. At the flame head (x = 150 mm, x = 170 mm, and x = 190 mm), the flame temperature further increases, and the ORZ almost disappears. In summary, these results show that the main factor affecting the re-circulation intensity is the flame part, and the ORZ is less influenced by the wall temperature conditions than the IRZ.

Analysis of temperature field and component field in large eddy simulation

The results of our study reveal that NH_3 propagates downward along the axial velocity and becomes enriched at the peak axial velocity position, as demonstrated in fig. 9(a). On the other hand, OH is predominantly formed in the IRZ, as illustrated in fig. 9(c), and subsequently mixed with the fresh mixture via the internal shear layer to oxidize NH_3 and H_2. The valley region of NO mole fraction is located exactly in the peak region of axial velocity, fig. 10(d), owing to the presence of unburned gas in this region.

Given that NO formation is sensitive to OH free radicals, the distribution of OH concentration in the IRZ corresponds with that of NO. Through the evaluation of temperature and OH mole fraction, the vortex flame structure of 50% NH_3/50% H_2 under lean condition f = 0.577 has been discussed, as displayed in figs. 8 and 9(c). Our analysis shows that the flame height is approximately 40 mm, which agrees with previous experimental results when f = 0.43 (~45 mm) and f = 0.52 (~42 mm) [12].

The temperature distribution within the flame zone is a critical factor in understanding the behavior of combustion processes. As discussed in figs. 9 and 10, under adiabatic conditions, the temperature is uniformly distributed within the flame zone, hovering around 1600 K. However, non-adiabatic conditions result in a non-uniform temperature distribution, causing a 50 K reduction in temperature compared to adiabatic conditions. The flame topology is characterized by the position with high OH concentration, indicating that an *M* flame topology is generated by eddy currents and bluff bodies.

Figures 9(c) and 10 illustrates that OH radicals collect at the flame front, suggesting that they are formed and consumed at the flame front. The outer edge of the OH profile corre-

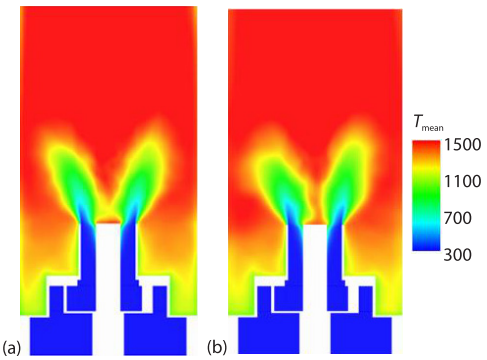

Figure 8. Comparison of axial average temperature at adiabatic and non-adiabatic wall conditions; (a) non-adiabatic axial average temperature and (b) adiabatic axial average temperature

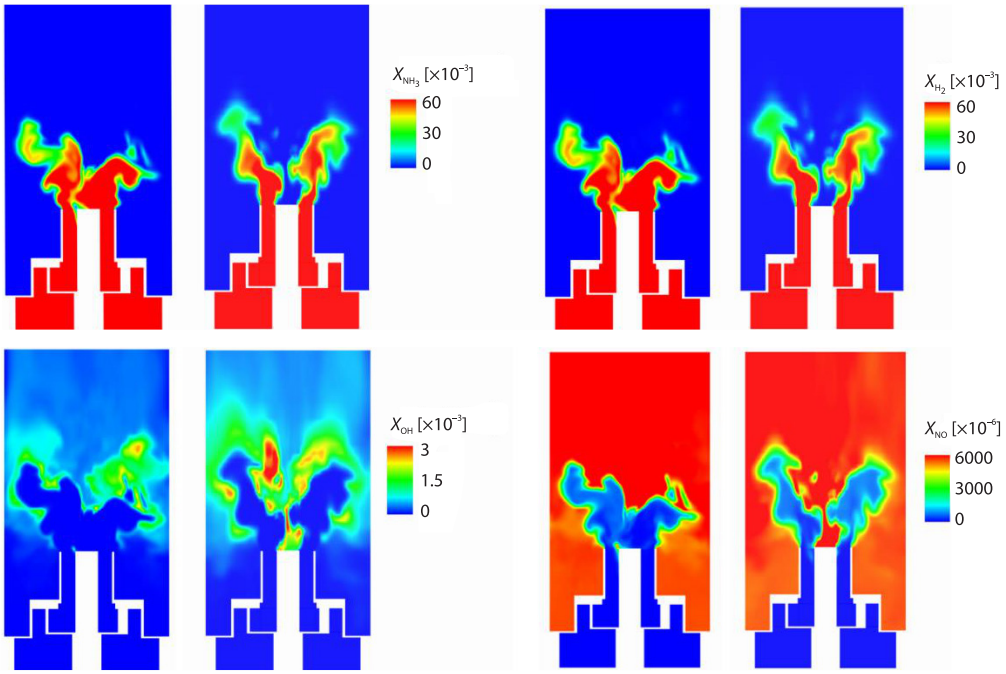

Figure 9. Comparison of transient components NH_3/H_2/OH/NO under non-adiabatic and adiabatic wall conditions

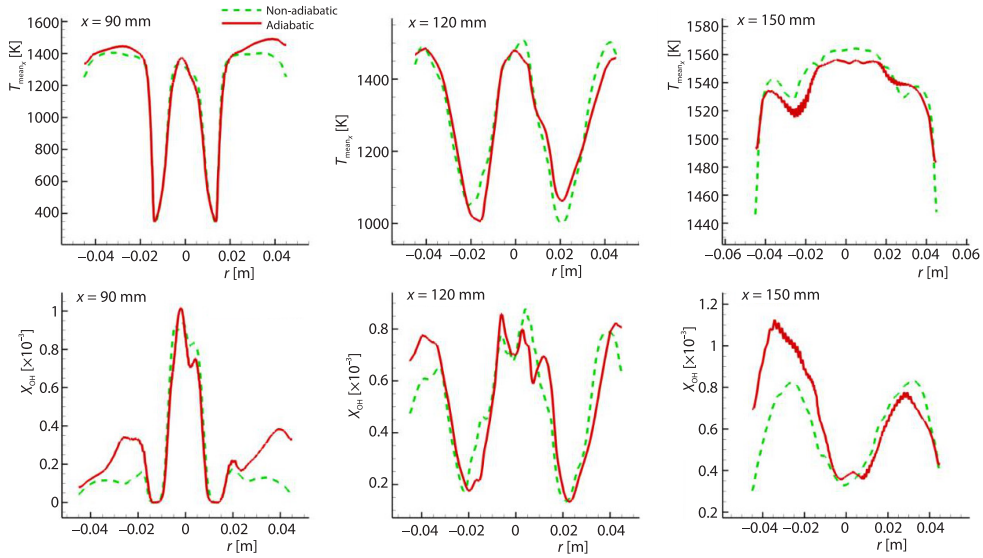

Figure 10. Comparison of the radial average temperature and OH components at different axial locations for non-adiabatic and adiabatic conditions, x = 90 mm, 120 mm, 150 mm

sponds to the velocity distribution and is irregular. Under adiabatic conditions, OH radicals exist throughout the entire combustion chamber downstream of the flame, while under non-adiabatic conditions, the OH content shows a gradient from the wall to the combustion chamber due

to heat loss. As a result, the temperature near the wall is lower than the temperature required for OH formation. The NH_3 propagates downward along the axial velocity and becomes enriched at the peak axial velocity position, while OH is primarily formed in the IRZ, mixed with the fresh mixture, and used to oxidize NH_3 and H_2. The valley region of NO mole fraction corresponds to the peak region of axial velocity due to the presence of unburned gas. The distribution of OH concentration in the IRZ is consistent with that of NO, which is formed due to OH free radicals.

In fig. 9, the mole fractions of NH_3, H_2, OH, and NO are represented, respectively. The reaction regions of NH_3 and H_2 are marked without blue, with the reaction region of H_2 being slightly larger than that of NH_3, consistent with the structure of a 1-D premixed free diffusion flame. Additionally, the concentration of NO in the ORZ is lower than that in the flame zone, primarily due to the dilution of NO concentration by cold air in the ORZ. The NO is predominantly produced at the front of the flame, where NH_3 is oxidized to HNO radicals, and OH radicals are enriched. Fuel NO is formed through the consumption of HNO and OH radicals. Finally, the distribution of NO under non-adiabatic conditions shows that NO is formed at the front of the flame, with the NO mole fraction and flame zone temperature under non-adiabatic conditions being lower than those under adiabatic conditions, indicating that fuel NO is sensitive to temperature.

Figure 11 shows the instantaneous distribution of the mole fractions of NH_3, H_2, and NO of the main species. Under inlet conditions, the molar ratio of NH_3 and H_2 is 1:1, re-

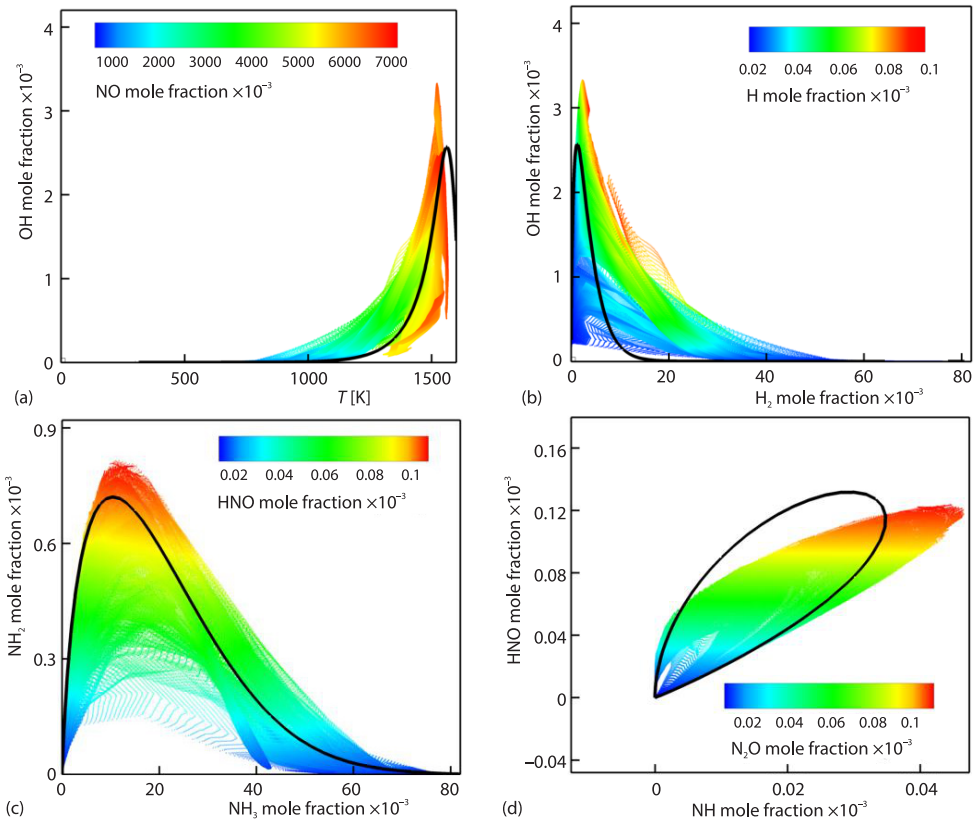

Figure 11. Scatter plots; (a) T-OH mole fraction, (b) H_2 mole fraction-OH mole fraction, (c) NH_3 mole fraction-NH_2 mole fraction, and (d) NH mole fraction-HNO mole fraction

sulting in almost the same distribution of NH_3 and H_2. In fig. 11, the scatter plots illustrate the relationships between the concentrations of various species and temperature at the flame front zone. It becomes apparent that at flame temperatures below 1600 K, thermal NO can be disregarded, and fuel NO is formed in the zone of high temperature and OH concentration, as demonstrated in fig. 11(a). The formation of OH radicals is highly temperature-sensitive, and thus flame temperature plays a pivotal role in determining fuel NO content. Moreover, a small amount of H_2 is involved in the formation of H and OH radicals, as depicted in fig. 11(b), which exhibits a positive correlation between H and OH concentrations.

In addition, the maximum concentrations of NH_2 and HNO are achieved when the NH_3 mole fraction is approximately $20 \cdot 10^{-3}$. Figure 11 (c) displays a positive correlation between NH_2 and HNO concentrations, which can be explained by the NH_3 decomposition path $NH_3 \rightarrow NH_i$ ($i = 0, 1, 2$) $\rightarrow$ HNO·N_2O is clearly correlated with NH_2 and HNO, as illustrated in fig. 11(d). The N_2O is the reduction product of NO, and HNO radical is a crucial intermediate species for the formation of NO. The NH_2, as an oxide, participates in the reduction of NO to form N_2O. When the HNO concentration is high and the NH_2 concentration is low, a large amount of NO will be generated, but NO cannot be reduced to N_2O due to the lack of NH_2. On the other hand, when the concentration of HNO and NH_2 is at a fixed proportion, these two radicals precisely promote the formation of N_2O.

Analysis of reflux intensity and comparison of large eddy simulation and chemical reactor network simulation and experimental results

In this paper, reflux intensity is defined as the proportion of reflux mass-flow to total mass-flow. The increase of reflux intensity can reduce NO emission. Therefore, the reflux intensity is an important parameter for the design of burner burning NH_3 fuel. The reflux intensity used by Cardiff University in the CRN numerical calculation is usually obtained by fitting the experimental value with the simulated value. In this paper, detailed flow field information can be obtained in LES, so relatively accurate reflux intensity can be obtained for future burner design and CRN numerical simulation.

According to the actual combustion situation, referring to the velocity field under LES under non-adiabatic conditions, the reflux intensity will reach a maximum of 65% in the flame development section, fig. 12. According to the aforementioned analysis, the reflux intensity will affect the re-reaction of the inhaled flue gas, and the NO in the flue gas will also be brought back to the reaction zone, which will increase the NO concentration in the reaction zone, so as to reduce the NO emission.

Based on the aforementioned analysis presented, the heat loss rate and reflux strength have been considered as important parameters in the context of CRN. In order to compare the numerical results obtained from CRN, LES, and experimental data, these two parameters have been applied in the CRN, and the results have been illustrated in fig. 13. It is worth noting that the NO concentrations predicted by LES are higher than those obtained in the experiment, whereas the CRN tends to underestimate the NO emission. It has been observed that the LES, which takes into account the non-adiabatic conditions, can predict the NO emission more accurately. On the other hand, the CRN, which considers the heat loss ratio and re-circulation strength calculated by LES, shows a good agreement with the experimental results.

The reason for this difference in the results can be attributed to the fact that the CRN analysis is only focused on the chemical reaction, which represents the ideal state of gas combustion. In contrast, the actual experiment involves other physical parameters and the error

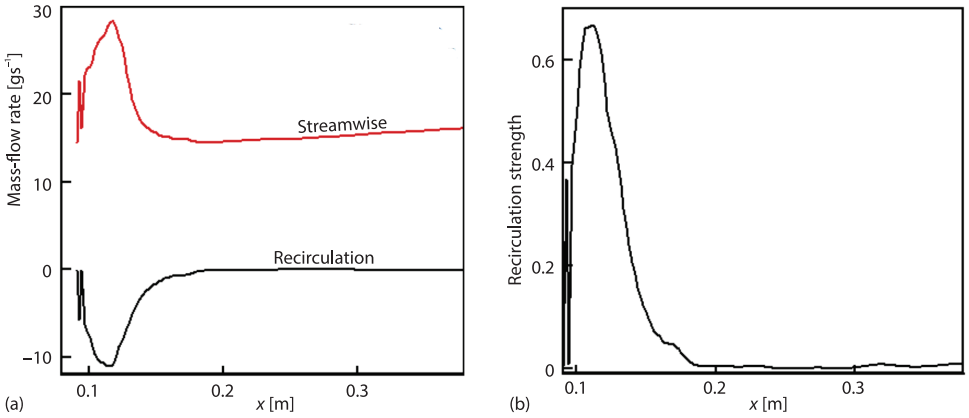

Figure 12. Mass-flow rate and re-circulation strength along the axis line for non-adiabatic condition; (a) mass-flow rate and (b) re-circulation strength

associated with the experiment itself. Furthermore, it has been observed that under large eddy simulation, the gas reaction on the adiabatic wall is more complete and the combustion temperature is higher, which leads to a greater NO emission than under non-adiabatic wall conditions. This can be attributed to the influence of the temperature field on gas reaction. Based on these findings, it can be concluded that reducing the reaction temperature can effectively reduce the NO emission.

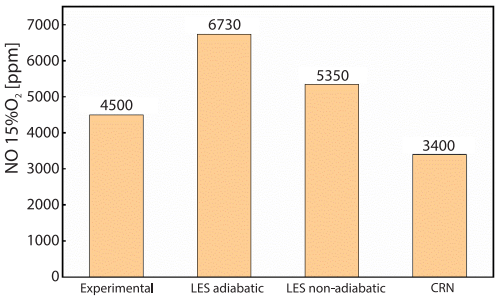

Figure 13. Comparison of amounts of NO emission (15% O_2) at $f = 0.577$ among LES results of adiabatic, non-adiabatic and CRN result, together with experiments

Conclusions

In the present investigation, a LES approach was employed utilizing the DTF model to examine the combustion characteristics of NH_3/H_2/air fields generated by a swirl burner. This study provides a detailed investigation of the underlying mechanisms of these combustion fields. The key findings of the study are summarized as follows.

- At lean condition $f = 0.577$, the flame height and flame thickness of 50% NH_3/50% H_2 were 40 mm and 0.8 mm, respectively.
- The re-circulation zone was located at the flame position, and the inner re-circulation strength played a decisive role in determining the total re-circulation strength. The maximum re-circulation strength of 0.65 was observed at the middle of the flame.
- The H_2 reacts first and generates a larger reaction zone than NH_3. Additionally, H and OH radicals are positively correlated, while there is some positive correlation between NH_2 and HNO. Furthermore, as the reduction product of NO, the concentration of N_2O is controlled by the concentration of HNO and NH_2 radicals.
- The OH radicals are predominantly formed in the inner re-circulation zone, while NO is produced at the flame front. Furthermore, NO emission is through the fuel NO path, which is highly sensitive to flame temperature.
- Reducing the combustion temperature can effectively reduce NO emission.

In summary, this study sheds light on the intricate details of NH_3/H_2/air combustion fields and provides valuable insights that can inform the development of more efficient and environmentally friendly combustion technologies.

Acknowledgment

The authors gratefully acknowledge the generous support provided by the Natural Science Foundation of China (NSFC) under Grant No. 91741117, and the High-tech Research Key Laboratory of Zhenjiang (No. SS2018002). The Support by the State Key Laboratory of Clean Energy Utilization (Open Fund Project No. ZJUCEU2022020) is also acknowledged. The authors also thank Prof. Agustin Valera-Medina and his team (Cardiff University, UK) for providing the experimental results.

References

[1] Chiuta, S., *et a*l., Reactor Technology Options for Distributed Hydrogen Generation Via Ammonia Decomposition: A Review, *Int. J. Hydrogen Energy*, *38* (2013), 35, pp. 14968-14991
[2] Michalsky, R., *et al*., Solar Thermochemical Production of Ammonia from Water, Air and Sunlight: Thermodynamic and Economic Analyses, *Energy*, *42* (2010), 1, pp. 251-260
[3] Yang, S. J., *et al*., Recent Advances in Hydrogen Storage Technologies Based on Nanoporous Carbon Materials, *Prog. Nat. Sci*., *22* (2012), 6, pp. 631-638
[4] Verkamp, F. J., *et al*., Ammonia Combustion Properties and Performance in Gas Turbine Burners, *Int. Symp. Combust*., *11* (1967), 1, pp. 985-992
[5] Lee, J. H., *et al*., Effects of Ammonia Substitution on Hydrogen/Air Flame Propagation and Emissions, *Int. J. Hydrogen Energy*, *35* (2010), 20, pp. 11332-11341
[6] Kumar, P., *et al.*, Experimental and Modelling Study of Chemical-Kinetics of Mechanisms for H_2-NH_3-Air Mixtures in Laminar Premixed Jet Flames, *Fuel*, *108* (2013), June, pp. 166-176
[7] Pratt, D. T., Performance of Ammonia Fired Gas Turbine Combustors, Report TR-9-TS-67-5, Solar, San Diego, Cal., USA, 1967
[8] Mathieu, O., *et al*., Experimental and Modelling Study on the Hightemperature Oxidation of Ammonia and Related NO_x chemistry, *Combust Flame*, *162* (2015), 3, pp. 554-570
[9] Hayakawa, A., *et al*., Experimental Investigation of Stabilization and Emission Characteristics of Ammonia/Air Premixed Flames in a Swirl Combustor, *Int. J. Hydrogen Energy*, *42* (2017), 19, pp. 14010-14018
[10] Han, X. L., *et al*., Experimental and Kinetic Modelling Study of Laminar Burning Velocities of NH_3/Air, NH_3/H_2/air, NH_3/CO/air and NH_3/CH_4/Air Premixed Flames, *Combust Flame*, *206* (2019), Aug., pp. 214-226
[11] Li, J., *et al*., Study on Using Hydrogen and Ammonia as Fuels: Combustion Characteristics and NO_x Formation, *Int. J. Energy Research*, *38* (2014), 9, pp. 1214-1223
[12] Valera-Medina, A., *et al*., Preliminary Study on Lean Premixed Combustion of Ammonia-Hydrogen for Swirling Gas Turbine Combustors, *Int. J. Hydrogen Energy*, *42* (2017), 38, pp. 24495-24503
[13] Valera-Medina, A., *et al*., Premixed Ammonia/Hydrogen Swirl Combustion under Rich Fuel Conditions for Gas Turbines Operation, *Int. J. Hydrogen Energy*, *44* (2019), 16, pp. 8615-8626
[14] Franco, M. C., *et al*., Characteristics of NH_3/H_2/Air Flames in a Combustor Fired by a Swirl and Bluff-Body Stabilized Burner, *Proc. Combust. Inst*., *38* (2021), 4, pp. 5129-5138
[15] Somarathne, K. D. K. A., *et al*., Numerical Study of a Low Emission Gas Turbine Like Combustor for Turbulent Ammonia/Air Premixed Swirl Flames with a Secondary Air Injection at High Pressure, *Int. J. Hydrogen Energy*, *42* (2017), 44, pp. 27388-27399
[16] Okafor, E. C., *et al.*, Towards the Development of An Efficient Low-NO_x Ammonia Combustor for a Micro Gas Turbine, *Proc. Combust. Inst.*, *37* (2018), 9, pp. 4597-4606
[17] Xiao, H., *et al*., The 3-D Simulation of Ammonia Combustion in a Lean Premixed Swirl Burner, *Energy Procedia*, *142* (2017), Dec., pp. 1294-1299
[18] Honzawa, T., *et al*., Predictions of NO and CO Emissions in Ammonia/Methane/Air Combustion by LES Using a Non-Adiabatic Flamelet Generated Manifold, *Energy*, *186* (2019), 115771
[19] Vigueras-Zuniga, M. O,. *et al.*, Numerical Predictions of a Swirl Combustor Using Complex Chemistry Fueled with Ammonia/Hydrogen Blends, *Energies*, *13* (2020), 2, 288

[20] Valera-Medina, A., *et al*., Ammonia, Methane and Hydrogen for Gas Turbines, *Energy Procedia*, *75* (2015), Aug., pp. 118-123
[21] ***, OpenFOAM 1.7.1. 2010. Available at: http://openfoam.org/version/1-7-1/, 2010
[22] Runyon, J., *et al*., Methane-Oxygen Flame Stability in a Generic Premixed Gas Turbine Swirl Combustor at Varying Thermal Power and Pressure, *Proceeding*s, ASME Turbo Expo, Montreal, Canada, 2015
[23] Butler, T. D., *et al.*, A Numerical Method for 2-D Unsteady Reacting Flows, *Proc. Combust. Inst*., *16* (1977), 1, pp. 1503-1515
[24] Angelberger, C., *et al*., Large Eddy Simulation of Combustion Instabilities in Turbulent Premixed Flames, *Proceedings of the Summer Program*, 1998, pp. 61-82
[25] Colin, O., *et al*., A Thickened Flame Model for Large Eddy Simulations of Turbulent Premixed Combustion, Physics of Fluids, *12* (2000), 7, pp. 1843-1863
[26] Wang, P., *et al*., A Detailed Comparison of Two Sub-Grid Scale Combustion Models Via Large Eddy Simulation of the PRECCINSTA Gas Turbine Model Combustor, *Combust Flame*, *164* (2016), Feb., pp. 329-345
[27] Xiao, H., *et al*., Modelling Combustion of Ammonia/Hydrogen Fuel Blends under Gas Turbine Conditions, *Energy Fuels*, *31* (2017), 8, pp. 8631-8642
[28] Mao, C. L., *et al.*, Laminar Flame Speed and NO Emission Characteristics of Premixed Flames with Different Ammonia-Containing Fuels, *J. Chem. Ind. Eng. (China)*, *72* (2021), 10, pp. 5530-5543
[29] Goodwin, D. G., *et al*., Cantera. http://www.cantera.org
[30] ***, ANSYS CHEMKIN PRO version 18.1. http://www.ansys.com/products/fluids/ansys-chemkin-proANSYS
[31] Rocha, R. C. D., *et al*., Chemical Kinetic Modelling of Ammonia/Hydrogen/Air Ignition, Premixed Flame propagation and NO emission, *Fuel*, *24*6 (2019), June, pp. 24-33
[32] Kumar, P., Meyer, T. R., Experimental and Modelling Study of Chemical-Kinetics Mechanisms for H_2-NH_3-Air Mixtures in Laminar Premixed Jet Flames, *Fuel*, *108* (2013), June, pp. 166-176

Paper submitted: November 23, 2023
Paper revised: June 27, 2024
Paper accepted: December 18, 2024